FATIGUE DESIGN OF PRESTRESSED CONCRETE BRIDGES UNDER SHEAR

Frederik Teworte, Institute of Structural Concrete, RWTH Aachen University, Germany
Josef Hegger, Institute of Structural Concrete, RWTH Aachen University, Germany

ABSTRACT

The demands on the load-carrying capacity of bridges have increased over the last decades due to higher traffic volume, especially by cause of commercial vehicles. Many existing bridge structures in Europe feature a high degree of prestressing and often contain less web reinforcement than the currently required minimum web reinforcement. Therefore, their shear resistance, originally determined based on the former code approaches (e.g. applying the principal tensile strength criterion), cannot be verified with the strut and tie models of the current code provisions.

Within a research program, the shear strength of prestressed concrete beams under cyclic loading has been investigated. Altogether, 42 tests on I-shaped and T-shaped beams without shear reinforcement and with low shear reinforcement ratios were performed. Based on the sustained cycles without failure, modified approaches for shear fatigue in terms of Goodman-Diagrams according to the principal tensile strength criterion have been developed. This paper describes the fatigue behavior and the modified approaches for the shear fatigue evaluation. The approaches may not only be used to assess the capacity of existing bridges, but also in the design of new prestressed constructions. The application to bridge structures is presented.

Keywords: Bridges, Design, Assessment, Shear, Fatigue, Prestressed

INTRODUCTION

Bridges are an important element of the infrastructure within the road network. The demands on the load-carrying capacity of bridges have increased over the last few decades due to higher traffic volume, especially by cause of commercial vehicles. Many existing bridge structures in Germany built in the 1960s and 1970s were designed for lower traffic loads[1] applying the principal tensile strength criterion[2,3] for shear. These structures typically feature a high degree of prestressing and low shear reinforcement ratios. In addition to the verification of the shear strength under static loading in the ultimate limit state, the shear fatigue resistance under service loads must be proved. Due to the reduction of the calculated shear resistance within the different code provisions, the shear capacity of the respective structures is often substandard according to the strut and tie models of the current design rules[4]. Since shear failure of the existing structures has not been observed so far, they are obviously able to carry the actual loads.

To investigate the number of cycles until failure and the failure indication (e.g. crack development) of prestressed concrete beams, fatigue tests on beams without shear reinforcement[5] (13 beams) and with low shear reinforcement ratios[6] (14 beams) were performed at the Institute of Structural Concrete at RWTH Aachen University. Within the test program, the influence of the shear reinforcement ratio, the prestressing, the maximum load and the load range were investigated. The test beams were designed referring to the conditions of existing bridges. A review of bridges built in the 1960s and 1970s was carried out to determine typical structures found in the German highway network, particularly to determine the appropriate cross-section geometry, degree of prestressing, and longitudinal and transverse reinforcement ratios. For these identified structures, static calculations with different load models were performed in order to obtain reasonable load regimes.

The present paper describes the fatigue behavior and crack development of I-shaped and T-shaped beams without shear reinforcement. Modified approaches for the shear fatigue evaluation based on the principal tensile strength criterion are presented along with their application to a typical bridge structure.

SHEAR DESIGN

The shear fatigue design of concrete bridges in Germany is performed according to the German Building code “DIN Fachbericht 102”[4], which is based on Eurocode 2. Since the shear strength under cyclic loading is defined depending on the static shear strength, the corresponding code provisions of the current and former design rules (DIN 4227[2]) are briefly described in the following.

The static shear design according to DIN 4227[2] was based on the limitation of the principal tensile stresses. The concrete shear stresses τ_{xy} and the longitudinal stresses σ_x were determined for various longitudinal sections at different heights under the relevant

load combination (figure 1). Assuming an uncracked section and a plane state of stress, the occurring principal tensile stresses σ_I can be calculated according to equation (1).

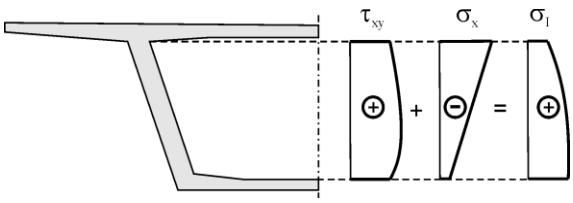

$$\sigma_I = \frac{1}{2}\left(\sigma_x + \sigma_y\right) + \sqrt{\left(\frac{\sigma_x - \sigma_y}{2}\right)^2 + \tau_{xy}^2} \quad (1)$$

Fig. 1 Schematic stress distribution within the web of a prestressed box girder

If σ_I exceeded the permitted maximum value, shear reinforcement was required. The maximum allowable value for pure shear in the ultimate limit state varied between 3.2 MPa (0.46 ksi) and 4.8 MPa (0.70 ksi), depending on the concrete's compressive strength.

The mean static shear strength of members without shear reinforcement $V_{Rm,ct}$ according to DIN Fachbericht 102[4] can be determined by equation (2). The value depends on the longitudinal reinforcement ratio ρ_l, the characteristic concrete compressive strength f_{ck}, the axial longitudinal concrete stress σ_c, the web width b_w, the effective depth d and κ considering the size effect. SI-units must be applied for each of the variables. To evaluate the performed tests, all equations are calculated with mean values concerning the material properties as well as the empirical factor. Hence, compared to the prescribed empirical factor $0.15/\gamma_c$ for design purposes[4] ($\gamma_c = 1.5$), a value of 0.2 is applied[7].

$$V_{Rm,ct} = \left(0.2 \cdot \kappa \cdot \left(100 \cdot \rho_l \cdot f_{ck}\right)^{1/3} - 0.12 \cdot \sigma_c\right) \cdot b_w \cdot d \quad (2)$$

Equation (2) may be used both in regions with and without flexural cracks. In contrast, $V_{Rm,ct}$ according to equation (3) may only be applied in regions featuring no flexural cracks in the ultimate limit state under static loading. Due to prestressing, a member may remain partially uncracked. In the case of existing highly prestressed bridges built in the 1960s and 1970s, equation (3) commonly leads to increased calculated values for $V_{Rm,ct}$ compared to equation (2). It considers the mean concrete tensile strength f_{ctm} and is based on the principal tensile strength criterion. The value f_{ctm} in SI-units according to the current code provisions[4] can be determined as $0.3 \cdot f_{ck}^{(2/3)}$applying the concrete compressive strength.

$$V_{Rm,ct} = \frac{I \cdot b_w}{S} \cdot \sqrt{f_{ctm}^2 - \sigma_c \cdot f_{ctm}} \quad (3)$$

To account for the load level dependent fatigue strength of unreinforced concrete, the shear fatigue strength (equation (4)) depends on the ratios of the applied shear load under maximum load ($V_{Ed,max}$) and minimum load ($V_{Ed,min}$) and the static shear strength ($V_{Rd,ct}$). Therefore, the design value of the static shear strength $V_{Rd,ct}$ is of major importance. According to the current design rules, $V_{Rd,ct}$ referring to equation (2) has to be applied as reference strength for shear fatigue; the shear strength according to equation (3) may not

be used. Equation (4) describes an envelope in a modified Goodman-Diagram for a defined number of cycles allowing for a graphical proof (figure 2).

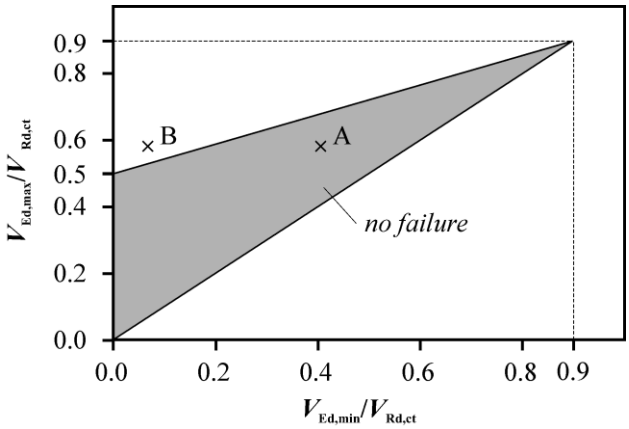

$$\frac{|V_{Ed,max}|}{|V_{Rd,ct}|} \leq 0.5 + 0.45 \frac{|V_{Ed,min}|}{|V_{Rd,ct}|} \leq 0.9 \qquad (4)$$

Fig. 2 Goodman-Diagram for shear fatigue design according to current design rules[4]

If a load combination lies within the enclosed grey shaded area (e.g. point A), no failure due to shear fatigue is expected. If the maximum load remains constant and the amplitude is increased by reducing the minimum shear force, the load combination moves further left in the diagram. When a point lies outside the shaded area (e.g. point B), a shear fatigue failure is predicted.

EXPERIMENTAL INVESTIGATIONS

The experimental program consisted of fatigue tests on prestressed concrete beams without shear reinforcement and with low shear reinforcement ratios. The shear reinforcement ratio of the beams with stirrups varied between 0.15 % and 0.33 %. The lower value refers to the required minimum shear reinforcement ratio according to the current German design rules[4], which corresponds well with the minimum transverse reinforcement ratio of 0.12 % according to AASHTO specifications[8]. The cyclic loading led to gradual stirrup fractures accompanied by a distinct increase of deformations and crack widths over a period of at least a few hundred thousand cycles before the beam failed. Therefore, a pronounced failure indication under cyclic loading can be assumed for superstructures with shear reinforcement ratios greater than the required minimum shear reinforcement ratio. More information about the tests on beams with a low amount of shear reinforcement is given in a previous paper[6,9]. The present paper describes the investigations on members without shear reinforcement.

TEST BEAMS

The test beams can be categorized depending on their cross-section geometry into tests on I-shaped and T-shaped beams (figure 3). The I-shaped beams were designed to fail due to diagonal cracking in the web, independent of flexural cracks. In contrast, in the shear loaded area of the T-shaped beams, flexural tensile stresses and cracks develop at

the soffit before failure. Thus, the influence of flexural tensile stresses on the crack development and the shear fatigue strength could be investigated.

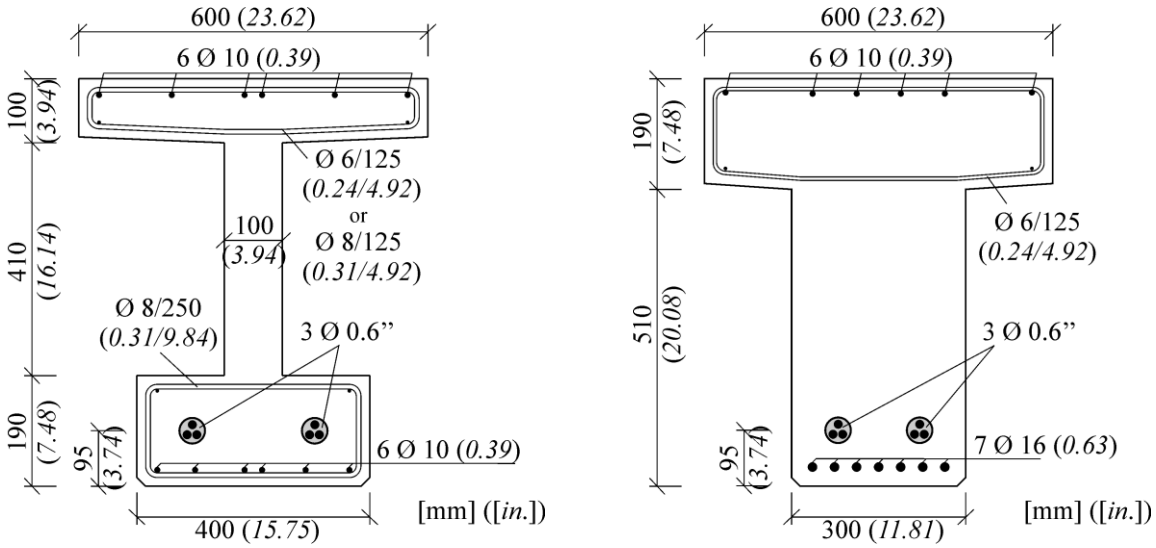

Fig. 3 Cross-sections of the I-beams (left) and T-beams (right)

The I-beams (I-O-1 till I-O-6) have a height of 700 mm (27.56 in.) and a web width of b_w = 100 mm (3.94 in.). While the web in the shear loaded area did not contain any stirrups, closed stirrups were placed in the top and bottom flanges to carry the shear forces between web and flanges. Prestressing was provided by two straight tendons at a distance of 95 mm (3.74 in.) from the soffit. Each tendon contained three 0.6” strands (St 1570/1770, $f_{p0,1k}$ = 1500 MPa), with a total area of A_p = 4.2 cm² (0.65 in.²). The cross-section of the non-prestressed longitudinal reinforcement (f_{yk} = 500 MPa) in the bottom flanges amounted to 4.71 cm² (0.73 in.²). This equals a longitudinal reinforcement ratio of 0.78 % assuming an effective depth of d = 605 mm (23.82 in.). In order to ensure that the beams could be lifted practically and to account for possible cracking at the top fiber while stressing the tendons, longitudinal reinforcement with a diameter of 10 mm (0.39 in.) was placed in the top flange.

The height of the T-beams (T-O-1 till T-O-6) amounted to 700 mm (27.56 in.) and was identical to that of the I-beams. The tendons as well as the stirrups in the flanges also did not differ from those used in the I-beams. Due to the greater web width of 300 mm (11.81 in.), the total area of the longitudinal reinforcement was increased to 14 cm² (2.17 in.²) so that the longitudinal reinforcement ratio remained constant. In the middle of the 6.5 m (255.9 in.) long beams over a length of 2.0 m (78.7 in.) closed stirrups were placed due to testing in two parts (see figure 4).

The applied prestressing forces were continuously measured with a load cell placed at the fixed anchor of one tendon. Assuming identical forces in both tendons, the prestressing forces $P_{m,tm}$ for each beam are given in table 1 as time-averaged values. The upper value results in a concrete compressive stress σ_{cp} at the centroidal axis of 3.7 MPa (0.54 ksi), corresponding to the stresses of strengthened bridges with external post-tensioning. The

lower values are within the range of those found in existing unstrengthened bridges. The concrete properties were determined for each beam. Since the obtained values did not show a significant increase throughout the test period, the time-averaged mean values of the concrete properties are used for further calculations. In table 1, the respective mean values of the compressive cylinder strength $f_{cm,cyl,tm}$ (150×300 mm, 5.9×11.8 in) and the uniaxial concrete tensile strength $f_{ctm,tm}$ are given. The tensile strength was determined on drilled cores (44×88 mm, 1.73×3.46 in) taken from separately cast specimens. The uniaxial force was applied via steel plates that were glued onto the plane surfaces with epoxy. The ready-mix concrete was designed to develop a compressive strength between 34 MPa (4.93 ksi) and 38 MPa (5.51 ksi) during the cyclic tests, lying in the lower scatter band compared to existing bridges.

Table 1: Prestressing forces, concrete properties and calculated static shear strengths

Beam No.	$P_{m,tm}$ kN/*kip*	σ_{cp} MPa/*ksi*	$f_{cm,cyl,tm}$ MPa/*ksi*	$f_{ctm,tm}$ MPa/*ksi*	$V_{Rm,ct}$ (2) kN/*kip*	$V_{Rm,ct}$ (3) kN/*kip*	$V_{um,MCFT}$ kN/*kip*
I-O-1	663/*149*	-3.72/*-0.54*	39.7/*5.76*	3.2/*0.46*	85/*19*	247/*56*	220/*49*
I-O-2	669/*150*	-3.77/*-0.55*	34.3/*4.97*	3.1/*0.45*	82/*18*	239/*54*	215/*48*
I-O-3	187/*42*	-1.05/*-0.15*	36.4/*5.28*	3.3/*0.48*	64/*14*	167/*38*	146/*33*
I-O-4	437/*98*	-2.45/*-0.36*	36.0/*5.22*	2.8/*0.41*	74/*17*	192/*43*	173/*39*
I-O-5	320/*72*	-1.80/*-0.26*	29.4/*4.26*	2.9/*0.42*	65/*15*	176/*40*	159/*36*
I-O-6	290/*65*	-1.62/*-0.23*	28.8/*4.18*	2.5/*0.36*	63/*14*	154/*35*	139/*31*
T-O-1	920/*207*	-3.47/*-0.50*	41.0/*5.95*	3.1/*0.45*	250/*56*	-*	405/*91*
T-O-2	616/*138*	-2.32/*-0.34*	37.5/*5.44*	3.0/*0.44*	220/*49*	-*	328/*74*
T-O-3R	516/*116*	-1.94/*-0.28*	37.7/*5.47*	2.6/*0.38*	212/*48*	-*	283/*64*
T-O-3	416/*94*	-1.58/*-0.23*	37.1/*5.38*	3.2/*0.46*	203/*46*	-*	292/*66*
T-O-4	485/*109*	-1.83/*-0.27*	36.4/*5.28*	2.5/*0.36*	207/*47*	-*	270/*61*
T-O-5	485/*109*	-1.82/*-0.27*	37.5/*5.44*	3.0/*0.44*	209/*47*	-*	295/*66*
T-O-6	615/*138*	-2.32/*-0.34*	34.8/*5.05*	2.6/*0.38*	215/*48*	-*	307/*69*

* cannot be calculated since flexural stresses at soffit exceed concrete tensile strength in ultimate limit state

$f_{cm,cyl,tm}$ = mean compressive cylinder strength; $P_{m,tm}$ = mean prestressing force; $\sigma_{cp} = P_{m,tm}/A_c$; $f_{ctm,tm}$ = mean concrete tensile strength

Based on the measured concrete properties and prestressing forces, the mean static shear strengths $V_{Rm,ct}$ according to equations (2) and (3) have been determined (table 1). The value $V_{Rm,ct}$ according to equation (3) depends on the longitudinal and shear stresses, and varies over the height of the beam. Hence, $V_{Rm,ct}$ has been determined in various layers of the cross-section iteratively at a distance of 1 m (39.4 in) from the support. In the ultimate limit state, the flexural stresses at the soffit of the T-beams exceed the concrete tensile strength, so that $V_{Rm,ct}$ cannot be determined according to equation (3). The static shear strength according to the AASHTO bridge design specifications[8] is determined based on the modified compression field theory (MCFT). The mean ultimate shear strengths $V_{um,MCFT}$ of the test beams given in table 1 have been calculated with the program

Response 2000 applying the mean material properties and mean prestressing forces. Compared to the current design rules for concrete bridges[4] in Germany, this approach reveals greater shear strengths for both cross-section geometries. For the I-beams, $V_{um,MCFT}$ is in the range of the mean static shear strength according to the principal tensile strength criterion (equation 3).

TEST SETUP AND TEST PROCEDURE

The simply supported beams were tested under four-point bending in the first part of the test with a span of 6.0 m (236.2 in.) (figure 4, left). The cyclic loading was applied at a frequency between 3.5 and 6 Hz, depending on the beam deflection. After shear failure within one side of the beam, the cyclic test on the other side was continued under three-point bending. This second part of the test featured the same shear-span-to-depth ratio (a/d = 3.3). The damaged side was strengthened via steel rods serving as external shear reinforcement. Therefore, two shear crack zones could be investigated on every beam.

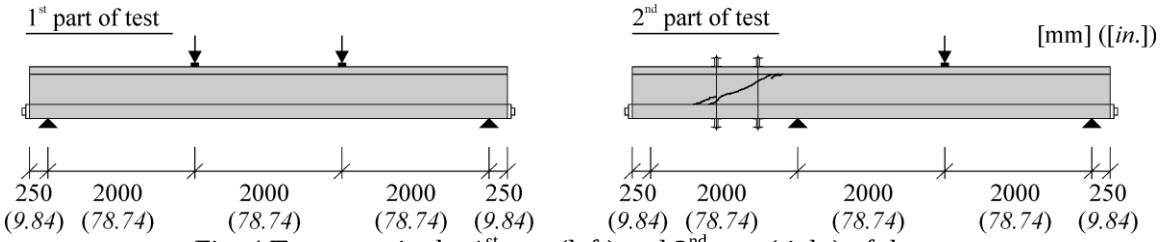

Fig. 4 Test setup in the 1st part (left) and 2nd part (right) of the test

If the beam did not fail after in general at least $1 \cdot 10^6$ cycles, the loads were changed so that different load regimes could be investigated on one beam. The investigated load combinations were defined based on the mean static shear strength $V_{Rm,ct}$ according to equation (3) and the ratio of the principal tensile stress and the concrete tensile strength $\sigma_I/f_{ctm,tm}$, respectively.

The applied shear loads under maximum load varied between 28 % and 79 % of the static shear strength, leading to principal stresses $\sigma_{I,max}$ of 0.5 MPa (72.5 psi) to 2.2 MPa (319.1 psi). This equals a utilization of the concrete tensile strength of approximately 15 % to 69 %. The applied minimum shear forces varied between 12 % and 69 % of the static shear strength. A cyclic shear failure of the I-beams was observed in five tests and the remaining static shear strength after previous cyclic loading was determined in five additional tests. In two tests, a static shear failure occurred. Due to the distinct bending and shear crack development of the T-beams under cyclic loading in the first part of the test, three-point bending tests could not be performed for beams with this cross-sectional geometry. One beam failed due to cyclic shear failure and one beam was tested to failure statically after previous cyclic loading. Despite the distinct bending and shear crack development, five beams did not fail under the applied cyclic loads. The remaining static shear strength was not determined for these beams to prevent the testing machine and the measuring equipment from being damaged due to the brittle failure. More detailed information on the applied load regimes, corresponding cycles and observed types of failure is given in a previous paper[5].

TEST RESULTS

The following briefly summarizes the failure indication with increasing number of cycles for both cross-sectional geometries. Furthermore, the performed tests are compared to the current code provisions[4] for shear fatigue of prestressed concrete beams without shear reinforcement.

FATIGUE BEHAVIOR

The I-beams failed independently of the type of loading (cyclic, remaining static shear strength) due to diagonal cracking in the web. Figure 5 shows typical crack patterns after failure of both sides of the beam. With increasing number of cycles, beam I-O-4 featured several short cracks in the web with crack widths less than 0.05 mm (0.002 in.). These cracks feature a smaller inclination than the critical shear crack leading to cyclic shear failure. Due to the lack of stirrups in the web, the cyclic and static shear failure by diagonal cracking occurred in a brittle manner without prior visible indication.

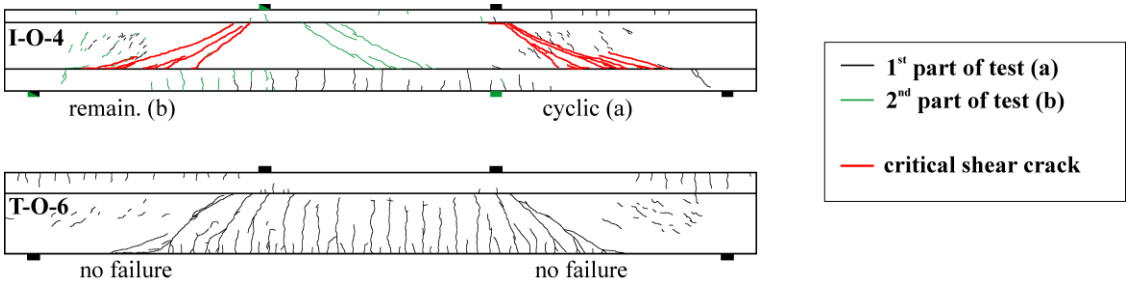

Fig. 5 Typical crack patterns of I-beams and T-beams

The T-beams without shear reinforcement featured bending cracks as well as inclined shear cracks between load introduction and support (figure 5). Despite the distinct bending and shear crack development, five beams did not fail under the applied loads.

In order to investigate the crack initiation before failure with increasing number of cycles, strain gauges and displacement transducers (LVDT) were used. As an example, the displacement of measuring point R2D within the last approximately 2,000 cycles of test I-O-4a is given in figure 6 (left). The LVDT was placed within the web almost perpendicular to the shear crack that suddenly developed after $4.013 \cdot 10^6$ cycles with a crack width of approximately 2.0 mm (0.08 in.). A second diagonal crack within the measuring range of the LVDT occurred after another 300 cycles, leading to shear fatigue failure of the beam after $4.502 \cdot 10^6$ cycles.

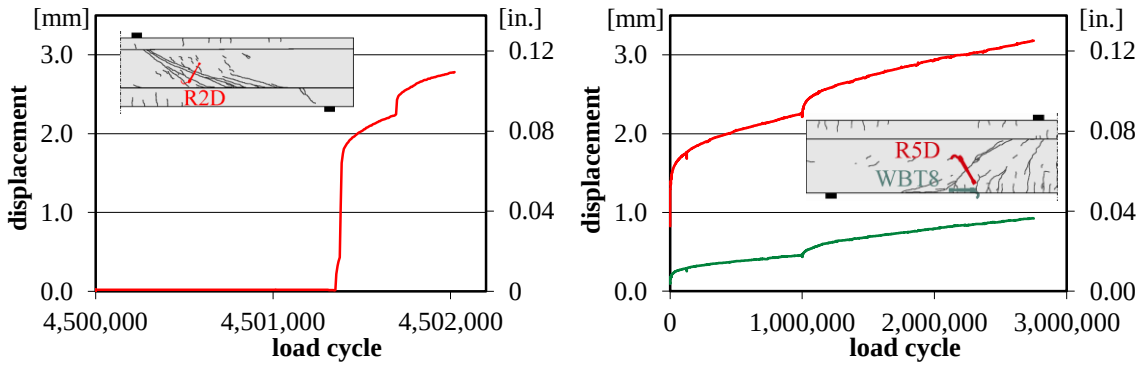

Fig. 6 Crack width under maximum load in test I-O-4a (left) and T-O-6a (right)

The crack development of the T-beams under cyclic loading differs from the I-beams' because of the different ratio of longitudinal stresses and shear stresses. In figure 6 (right), the flexural crack and shear crack development under maximum load in test T-O-6a is given. The flexural crack width (WBT8) after the first cycle amounted to 0.11 mm (0.004 in.) and increased continuously with increasing number of cycles up to 0.93 mm (0.04 in.) at the end of the test. At the beginning of a new shear load amplitude after $1 \cdot 10^6$ cycles with unchanged maximum load, a considerable increase in crack width occurred, reducing with further test progression. This also concerns the corresponding shear crack width (R5D). Despite a shear crack width of more than 3 mm (0.11 in.) at the end of the test, the beam was able to carry the applied loads.

SHEAR FATIGUE STRENGTH

To compare the test results with the current code provisions[4] for shear fatigue, the Goodman-Diagram for constant shear load amplitudes is used. For the comparison in figure 7, all load combinations that could be sustained for at least $1 \cdot 10^6$ cycles without shear fatigue failure are considered. Since each beam was exposed to variable shear load amplitudes, the load combinations that caused shear fatigue failure are not plotted.

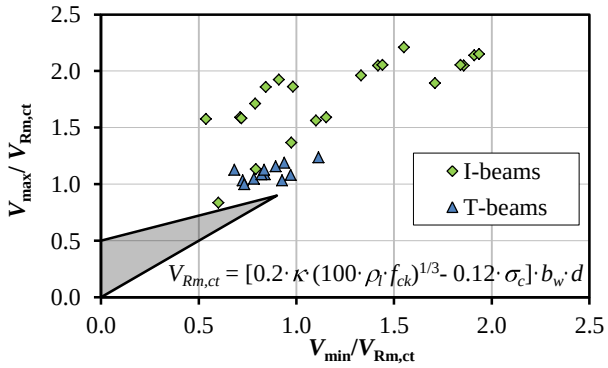

Fig. 7 Comparison of test results and code provisions for shear fatigue (Goodman-Diagram)

All investigated load combinations lie outside the envelope (shaded grey), which indicates the permitted load combinations. Hence, a shear fatigue failure or even a static shear failure during the first cycle ($V_{max}/V_{Rm,ct} > 1.0$) is predicted incorrectly. Consequently, the reference shear strength according to equation (2) underestimates the

static shear strength of the investigated I-beams and T-beams, as well as the number of sustained cycles without fatigue failure.

MODIFIED APPROACHES FOR SHEAR FATIGUE

Based on the sustained cycles without failure, two different approaches for the shear fatigue of prestressed beams without shear reinforcement have been developed. The first approach limits the permitted shear load amplitudes, while the second approach constrains the permitted principal tensile stresses under cyclic load.

Since the static shear strength according to equation (2) underestimates the load bearing capacity of the investigated I-beams considerably, it is not appropriate as reference strength for the limitation of the shear load amplitude. Therefore, contradicting the current code provisions[4], a limitation of the permitted shear loads under cyclic loading based on the principal tensile strength criterion (equation (3)) is proposed for the shear fatigue evaluation of I-beams. The approach may only be applied to regions without flexural tensile stresses at the height of the end of the web, corresponding to the conditions of the tested beams. An application to T-beams is not possible, as the value $V_{Rm,ct}$ according to equation (3) cannot be determined in the ultimate limit state. With regard to these requirements, the Goodman-Diagram for $N = 1 \cdot 10^6$ cycles has been developed (figure 8, left). The plotted load combinations could be sustained at least for $1 \cdot 10^6$ cycles without shear fatigue failure, and are identical to those considered in figure 7. For the evaluation of the shear fatigue strength, the maximum shear load V_{max} and the respective shear load amplitude ΔV must be limited. The permitted load combinations (shaded grey) are defined based on the performed tests. The maximum shear load may not exceed 75 % of the mean static shear strength $V_{Rm,ct}$ and ΔV must be smaller than $1/3 \cdot V_{Rm,ct}$. Hence, seven out of 21 load combinations that did not lead to shear fatigue failure lie outside the defined envelope and their sustained number of cycles without failure is underestimated. The dashed lines represent the shape of the envelope for cyclically loaded concrete under compression and shear[4], respectively.

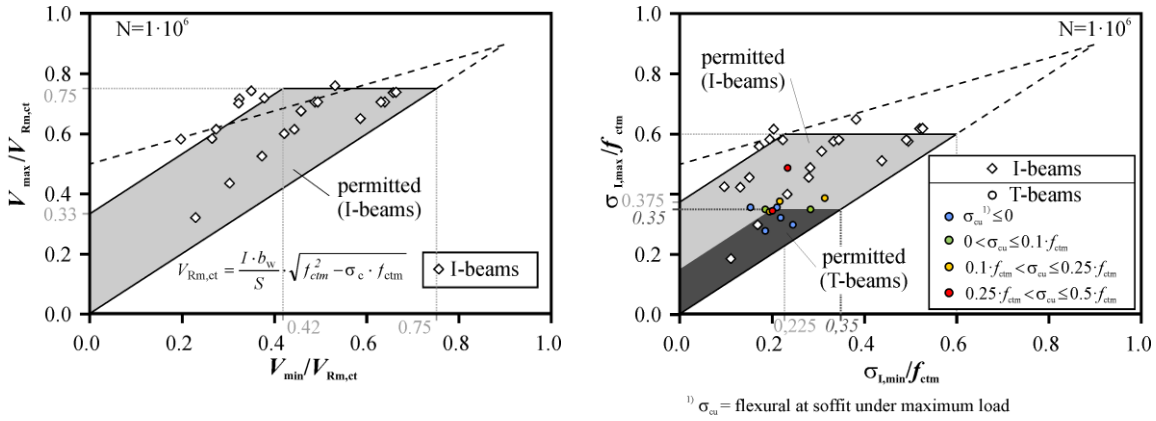

Fig. 8 Proposed limitation of shear loads (left) and principal tensile stresses (right)

An alternative approach for the shear fatigue evaluation is the limitation of the principal tensile stresses σ_I under cyclic loading. The longitudinal stresses and shear stresses under the applied fatigue loads differ from the ultimate limit state under static loading. Therefore, the ratio $V/V_{Rm,ct}$ and σ_I/f_{ctm} is not identical for the same load combination. In contrast to the limitation of shear loads, the ratio of the tensile stresses and the concrete tensile strength under maximum and minimum load is used in the Goodman-Diagram (figure 8, right). Since the beams remain uncracked or only features small flexural tensile stresses under fatigue loading, this approach may be applied to both I-shaped and T-shaped beams.

The principal tensile stress under maximum load $\sigma_{I,max}$ of the I-shaped beams may not exceed 60 % of the mean concrete tensile strength f_{ctm}. The permitted principal tensile stress under minimum load $\sigma_{I,min}$ must be limited so that the principal tensile stress amplitude $\Delta\sigma_I$ is smaller than $0.375 \cdot f_{ctm}$. This definition of the permitted load combinations (light grey) underestimates the shear fatigue strength of six of the 21 load combinations, which did not cause fatigue failure.

The permitted tensile stresses of prestressed T-beams are shown in figure 8 (right) (dark grey). The plotted load combinations that did not lead to shear fatigue failure before $1 \cdot 10^6$ cycles in the tests are divided into four groups, depending on the flexural stresses σ_{cu} at the soffit of the beam in the middle between load introduction and support. Due to the limited test data, the flexural stress at the soffit of the beam under cyclic loading should be limited to $0.1 \cdot f_{ctm}$. The principal tensile stress under maximum load $\sigma_{I,max}$ may not exceed $0.35 \cdot f_{ctm}$ and the permitted maximum value $\Delta\sigma_I$ amounts to 15 % of the concrete tensile strength. According to this definition, the number of sustained cycles without failure is underestimated for six of the 12 investigated load combinations.

APPLICATION TO BRIDGE STRUCTURES

Existing bridges built in the 1960s and 1970s typically have a high degree of prestressing. Therefore, these structures generally do not exhibit inclined web shear cracking under service loads, which have to be applied in the fatigue verification. Consequently, the proposed fatigue evaluation is primarily based on the verification of the bridge structure as an uncracked prestressed member without shear reinforcement. In the following, the application of the developed approach to a typical existing bridge type of the German road network is presented.

The 174.5 m (572 ft.) long road bridge was built in the 1960s with 7 spans varying between 17.5 m (57 ft.) and 30 m (98 ft.). Each direction features a separate prestressed superstructure (figure 9). The box-girder has a total height of about 1.8 m (5.9 ft.) and a width of 11.3 m (37 ft.). Within the 0.6 m (1.96 ft.) wide webs, stirrups with a steel grade IIIa (f_{yk} = 420 MPa) were placed leading to shear reinforcement ratios between 0.23 % and 0.56 %, depending on the longitudinal section.

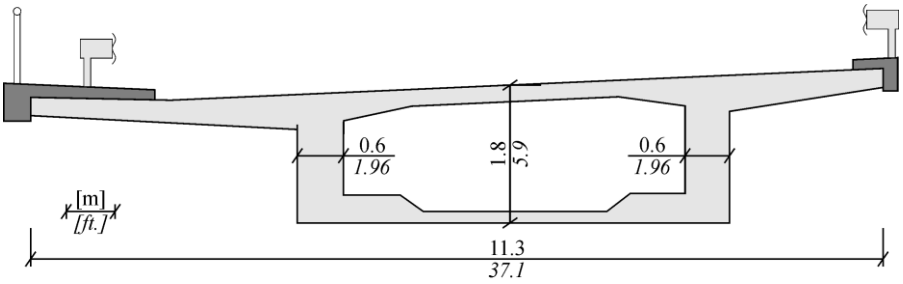

Fig. 9 Cross-section of prestressed box-girder bridge

According to the German design code[4], the shear fatigue verification for new structures has to be performed under the frequent load combination, which assumes a recurrence of up to 300 times a year (equation (5)). For the evaluation of existing bridges, the loads experienced to date and the planned remaining service life have to be considered. Conservatively based on the current state of knowledge, the frequent load combination applied in the design of new structures is also used for the evaluation of existing bridges. The variable G_k represents the permanent actions (e.g. dead weight) and P_k the actions due to prestressing. The leading variable action $Q_{k,1}$ is multiplied by the combination factor ψ_1 and the other variable actions $Q_{k,j}$ by the combination factor ψ_2.

$$E_d = \sum_{j\geq 1} G_{k,j} + P_k + \psi_{1,1} \cdot Q_{k,1} + \sum_{i>1} \psi_{2,i} \cdot Q_{k,i} \tag{5}$$

To assess the cyclic shear strength of the box-girder, the dead weight, the imposed dead loads and the prestressing were considered. Furthermore, the variable actions due to temperature effects, settings of the foundations and traffic were applied. The relevant traffic load model[10] for shear fatigue is shown in figure 10. It consists of uniformly distributed loads (UDL) and a tandem system (TS) representing wheel or axle loads. In the first lane, the value q_{UDL} amounts to 9.0 kN/m² (1.31 psi), and in the second lane as well as the remaining area to 2.5 kN/m² (0.36 psi). The vertical loads Q_{TS} of the tandem system have to be applied in the first and second lane with values of 240 kN (54 kip) and 160 kN (36 kip) for each axis, respectively.

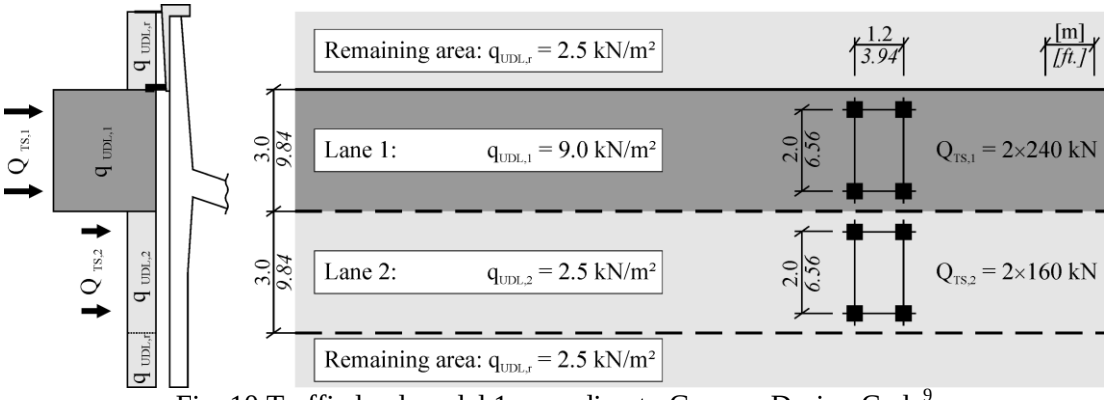

Fig. 10 Traffic load model 1 according to German Design Code[9]

The shear fatigue resistance of the bridge cannot be verified according to the current German design rules[4]. Therefore, the developed approach based on limiting the principal

tensile stresses is applied. In the following, the application is shown for two sections, located at a distance of 3.35 m (11 ft.) (section 1) and 3.55 m (11.6 ft.) (section 2) from an interior column (figure 11). The box girder exhibits a top flange (bridge deck slab) and a bottom flange (bottom slab), so that the permitted values for I-beams are used.

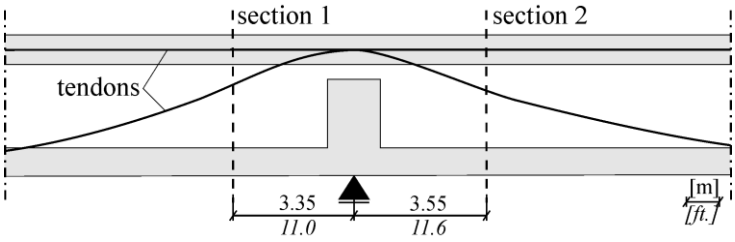

Fig. 11 Location of sections for shear fatigue evaluation at interior column

First, it is necessary to determine whether the developed approaches for shear fatigue of members without shear reinforcement may be applied to the structure by calculating the flexural stresses. Box girder bridges must remain uncracked within the web. Therefore, no flexural tensile stresses σ_x at the height of the end of the web are allowed. The flexural stresses are determined under the fatigue load combination according to equation (5). In figure 12, the stress distribution within the web in section 1 under the maximum design load is shown. At the top end of the web, the longitudinal stresses σ_x amount to -3.5 MPa (-508 psi) under the frequent load combination, so that the developed approach is applicable. Since in section 2 longitudinal compressive stresses occur at the top end of the web as well, the approach can also be applied there.

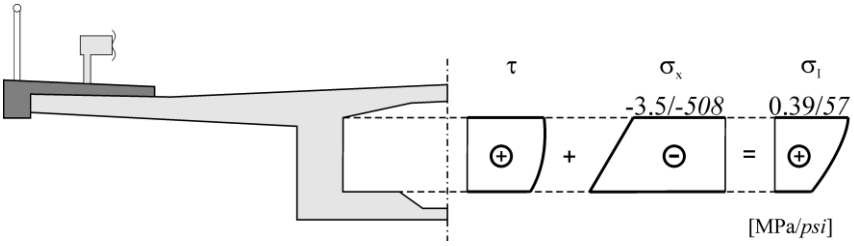

Fig. 12 Stress distribution under maximum design load within the web in section 1

In addition to the longitudinal stresses, the shear stresses τ and principal tensile stresses σ_I within the web over the height of the beam are given in figure 12. Referring to the former code provisions for concrete bridges[2], τ has been calculated in the middle of the web, considering the stresses due to shear and torsion. The principal tensile stresses have been determined according to equation 1, whereas vertical normal stresses in the web were neglected. The maximum design value of the principal tensile stress under the frequent load combination $\sigma_{I,max,Ed}$ in section 1 amounts to 0.39 MPa (57 psi). In addition to $\sigma_{I,max,Ed}$, the minimum principal tensile stress under the relevant load combination was determined in order to obtain the design value of the shear load amplitude $\Delta\sigma_{I,Ed}$. A summary of the calculated principal tensile stresses for both sections is given in table 2.

Table 2: Principal tensile stresses

	Section 1		Section 2	
	$\sigma_{I,max,Ed}$	$\Delta\sigma_{I,Ed}$	$\sigma_{I,max,Ed}$	$\Delta\sigma_{I,Ed}$
Design value E_d [MPa/*psi*]	0.39/*57*	0.22/*32*	0.52/*75*	0.22/*32*
Concrete resistance R_d [MPa/*psi*]	0.80/*116*	0.50/*73*	0.80/*116*	0.50/*73*
$\eta = E_d/R_d$	0.49	0.44	0.65	0.44

The concrete resistance R_d equals the permitted principal tensile stress under maximum load and the permitted stress amplitude, respectively. It depends on the design value of the concrete tensile strength f_{ctd}, which is determined referring to the guidelines for survey and redesign of bridges[11] and the current design code for concrete bridges[4]. Considering the partial safety factor for concrete γ_c, the value f_{ctd} amounts to $f_{ctd} = f_{ctk;0,05} / \gamma_c = 2.0 / 1.5 = 1.33$ MPa (193 psi). According to the experimental investigations on prestressed beams with shear reinforcement[6,9], a pronounced failure indication under cyclic loading can be assumed for beams with shear reinforcement ratios greater than the required minimum shear reinforcement ratio[4]. Therefore, the partial safety factor for reinforced concrete[4] $\gamma_c = 1.5$ is used. The characteristic concrete tensile strength $f_{ctk;0,05}$ corresponds to the existing compressive strength class C30/37 (f_{ck} = 30 MPa, 4.35 ksi).

The calculated maximum principal tensile stresses do not exceed the permitted value of 0.8 MPa (116 psi) ($0.6 \cdot f_{ctd}$), leading to ratios $\eta = E_d / R_d$ less than 1. In addition, the principal stress amplitudes $\Delta\sigma_{I,Ed}$ are smaller than the permitted maximum value of 0.5 MPa (73 psi) ($0.375 \cdot f_{ctd}$). Therefore, the shear fatigue resistance of the structure is verified in both sections by applying the developed approaches for prestressed beams without shear reinforcement under cyclic loading.

CONCLUSIONS

To investigate the number of cycles until failure and the failure indication (e.g. crack development) of prestressed concrete beams without shear reinforcement, fatigue tests on I-shaped and T-shaped beams were performed at the Institute of Structural Concrete at RWTH Aachen University. The beams were able to resist more cycles than predicted by the current German code provisions[4] for shear fatigue. The cyclic shear failure by diagonal cracking of the I-beams occurred in a brittle manner without prior visible indication. Despite the distinct bending and shear crack development of the T-beams, a failure under the applied loads was not observed in six tests. In one test, the T-beam failed under cyclic loading due to the sudden development of a diagonal crack. However, the performed tests on prestressed concrete beams with stirrups[6,9] indicate, that a pronounced failure indication under cyclic loading can be assumed for superstructures with shear reinforcement ratios greater than the required minimum shear reinforcement ratio[4,8].

Based on the sustained cycles without failure, two different approaches for shear fatigue of prestressed beams without shear reinforcement have been developed in terms of Goodman-Diagrams. The first approach limits the permitted shear load amplitudes, whereas the principal tensile strength criterion is applied to determine the static shear strength. The second approach restricts the permitted principal tensile stresses under cyclic shear. The approaches may be applied to I-beams in uncracked regions and T-beams with limited flexural stresses at the soffit.

The application of the developed approaches to a prestressed bridge structure in order to assess the shear strength under cyclic load has been presented. The cross-section generally does not feature inclined web shear cracking under service loads, which have to be applied in the fatigue verification. Therefore, the proposed fatigue evaluation is primarily based on the verification of the bridge structure as an uncracked prestressed member without shear reinforcement.

ACKNOWLEDGEMENTS

The investigations have been funded by the German Research Foundation "DFG" (reference HE 2637/12-1) and the Hessian Road and Traffic Administration "Hessen Mobil". The authors express their thanks to the DFG, Hessen Mobil and the members of the project committee for the constructive discussions. Furthermore, the authors would like to thank Mr. Doser (H+P Engineers, Aachen, Germany) for his contribution to the design example.

REFERENCES

1. DIN 1072, German Design Code "Road bridges - Actions on bridges", 1953.
2. DIN 4227, German Design Code "Prestressed concrete - Guidelines for design and construction", 1953.
3. BMV-Richtlinie, German Design Guideline: "Additional provisions to DIN 4227 for prestressed concrete bridges", 1969.
4. DIN Fachbericht 102, German Design Code "Concrete Bridges", 2009.
5. Teworte, Frederik, and Hegger, Josef, "Fatigue of prestressed beams without web reinforcement under cyclic shear," *Beton- und Stahlbetonbau*, V. 108, No. 1, Jan. 2013, pp. 34-46.
6. Teworte, Frederik, and Hegger, Josef, "Fatigue of prestressed beams with web reinforcement under cyclic shear," *Beton- und Stahlbetonbau*, V. 108, No. 7, Jul. 2013, pp. 475-486.
7. Deutscher Ausschuss für Stahlbeton (DAfStb), "Heft 600: Erläuterungen zu DIN EN 1992-1-1 und DIN EN 1992-1-1/NA (Eurocode 2)", (German Committee for Structural Concrete, issue 600: Comments on DIN EN 1992-1-1 and DIN EN 1992-1-1/NA (Eurocode 2)), Beuth Verlag, 2012.
8. American Association of State Highway and Transportation Officials (AASHTO), "AASHTO LRFD Bridge Design Specifications", 4th edition, 2007.
9. Teworte, Frederik, and Hegger, Josef, "Fatigue of Prestressed Concrete Beams with low Shear Reinforcement Ratios – Experimental Investigations," *18th IABSE Congress on Innovative Infrastructures*, Sept. 2012.

10. DIN Fachbericht 101, German Design Code “Actions on Bridges”, 2009.
11. Federal Ministry of Transport, Building and Urban Development, “Guidelines for Survey and Redesign of Bridges”, 2011.